(2)

Development of Garnet Films for Magnetostatic Wave Channelized Receivers

by

R.F. Belt and J.B. Ings

Final Report
October 1, 1989 - May 1, 1992
Contract No. N00014-89-C-2228

Airtron Division
Litton Systems Inc.
200 E. Hanover Ave.
Morris Plains, NJ 07950

June, 1992

Notices

NOTICES

The findings in this report are not to be construed as an official Department of the Navy position unless designated by other authorized documents.

The citation of trade names or names of manufacturers in this report should not be taken as official Government endorsement or approval of commercial products or services referenced herein.

When Government drawing, specifications, or other data are used for any purpose other than in connection with a definitely related Government procurement operation, the United States Government thereby incurs no responsibility nor an obligation whatsoever; and the fact that the Government may have formulated, furnished, or in any way supplied the said drawings, specifications, or other data, is not to be regarded by implication or otherwise as in any manner licensing the holder of any other person or corporation, or conveying any rights or permission to manufacture, use, or sell any patented invention that may in any way be related thereto.

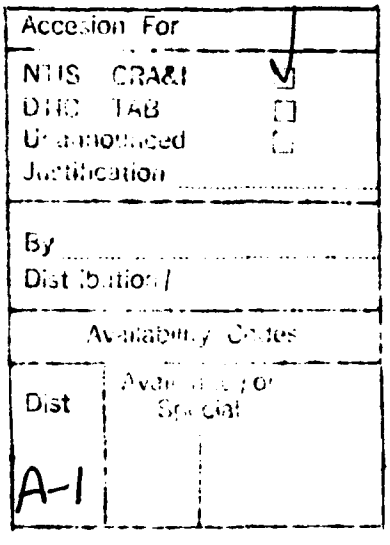

REPORT DOCUMENTATION PAGE

1a. REPORT SECURITY CLASSIFICATION Unclassified	1b RESTRICTIVE MARKINGS None
2a. SECURITY CLASSIFICATION AUTHORITY	3 DISTRIBUTION / AVAILABILITY OF REPORT Not limited
2b. DECLASSIFICATION / DOWNGRADING SCHEDULE	
4. PERFORMING ORGANIZATION REPORT NUMBER(S)	5. MONITORING ORGANIZATION REPORT NUMBER(S)
6a. NAME OF PERFORMING ORGANIZATION Airtron Division Litton Systems, Inc. 6b. OFFICE SYMBOL (*If applicable*)	7a. NAME OF MONITORING ORGANIZATION Naval Research Laboratory Department of the Navy
6c. ADDRESS (*City, State, and ZIP Code*) 200 E. Hanover Ave Morris Plains, NJ 07950	7b. ADDRESS (*City, State, and ZIP Code*) 4555 Overlook Ave, S.W. Washington, DC 20375-5000
8a. NAME OF FUNDING / SPONSORING ORGANIZATION Naval Research Laboratory 8b. OFFICE SYMBOL (*If applicable*)	9. PROCUREMENT INSTRUMENT IDENTIFICATION NUMBER N00014-89-C-2228 Code 3220 WB
8c. ADDRESS (*City, State, and ZIP Code*) Department of the Navy 4555 Overlook Ave, S.W. Washington, DC 20375-5000	10. SOURCE OF FUNDING NUMBERS PROGRAM ELEMENT NO. / PROJECT NO. PR65-9220-89 / TASK NO 65181N-0-1-96507 / WORK UNIT ACCESSION NO
11. TITLE (*Include Security Classification*) Development of Garnet Films for Magnetostatic Wave Channelized Receivers	
12. PERSONAL AUTHOR(S) R.F. Belt, and J.B. Ings	
13a. TYPE OF REPORT Final	13b. TIME COVERED FROM Oct 89 TO May 92
14. DATE OF REPORT (*Year, Month, Day*) 92-6-30	15. PAGE COUNT vii+43
16. SUPPLEMENTARY NOTATION None	

17. COSATI CODES			18. SUBJECT TERMS (*Continue on reverse if necessary and identify by block number*)
FIELD	GROUP	SUB-GROUP	Garnet Films, Channelizers, Magnetostatic Waves, Liquid phase epitaxy

19. ABSTRACT (*Continue on reverse if necessary and identify by block number*)

Single Crystal films of $Bi_{3-x}Lu_xFe_5O_{12}$ were grown by liquid phase epitaxy on one inch diameter wafers of GGG. Most compositions were centered about X=2.17 with dopants of Mg^{2+} to control the optical absorption. More than 100 experimental films were grown under a variety of growth conditions. The film properties were measured at Airtron and correlated with growth conditions. In addition, measurements of optical absorption, electrical resistivity, resonanc linewidth, and Faraday rotation were performed on selected samples. Microwave passband measurements were also conducted at University of Delaware and Westinghouse Research Laboratory to determine the suitability of our films for channelizer devices. Thus far an unknown problem with these films has prevented passband measurements equivalent to pure YIG films.

20. DISTRIBUTION / AVAILABILITY OF ABSTRACT ☒ UNCLASSIFIED/UNLIMITED ☐ SAME AS RPT. ☐ DTIC USERS	21. ABSTRACT SECURITY CLASSIFICATION Unclassified
22a NAME OF RESPONSIBLE INDIVIDUAL	22b. TELEPHONE (*Include Area Code*) / 22c. OFFICE SYMBOL

Table of Contents

List of Figures

List of Tables

Foreword

This final report describes a research effort on the preparation of $Bi_{3-x}Lu_xFe_5O_{12}$ garnet films by liquid phase epitaxy. The films have direct applications to magnetostatic wave (MSW) devices used in channelized receivers for microwave technology. The origins of this investigation are associated with work by the Optical Information and Signal Processing Group at the Naval Research laboratory. Dr. John N. Lee served as contract monitor and technical coordinator for the various program activities. The report describes research performed during the period of October 1, 1989 to May 1, 1992 under the issued contract number N00014-89-C-2228.

All film growth for this program was performed in the laboratories of Airtron Division of Litton Systems Inc., 200 E. Hanover Ave., Morris Plains, NJ 07950. The research was under the direction of Dr. Roger F. Belt with Dr. John B. Ings serving as senior scientist. Outside measurements were performed by Dr. J.C. Butler of the Electrical Engineering Department, University of Delaware, Newark, Delaware 19716. Thanks are also due to Professor J.J. Kramer of the University of Delaware and Dr. Sal Talisa of Westinghouse for helpful discussions on linewidth and passband microwave data. This report was prepared by Roger Belt and John Ings. It was released for distribution in July, 1992.

1.0 Introduction

The problem of intercepting and separating several time-coincident signals simultaneously can be solved by channelized receivers. The application of this technology to RF, microwave, and millimeter waves has been reviewed recently.(1) Particular attention has been given to magnetostatic wave (MSW) devices and phenomena.(2) The diffraction of guided optical waves in thin films of YIG by magnetostatic waves (MSW) is promising for large time-bandwidth signal processing devices in the 1-20 GHz range. Mode conversion between a TM and TE waveguide has also been demonstrated.(3) New applications for integrated-optic rf spectrum analyzers, deflectors, and switches appear to be possible. In order to increase the efficiency of these devices and decrease the interaction length to a few cm, it is essential to have a material with high Faraday rotation at the optical wavelength. In addition, for low loss microwave devices, the resonance linewidth must be as low as possible. The preparation of ferrimagnetic bismuth containing single crystal films of YIG offer one possible solution to the stringent material demands. However, great difficulty has been encountered in the routine preparation of these films and few research efforts have addressed the problems.

In 1988 Tamada and coworkers (4) were the first to investigate optical mode conversions induced by MSW in $(BiLu)_3Fe_5O_{12}$ films. A few years later Butler, et. al.(5) investigated some of the fundamental microwave and magneto-optic properties of Bi YIG films. In a continuing effort to develop high efficiency devices with the Lu containing films, this program examined the growth parameters more closely to attain high quality films on one inch diameter substrates. Samples obtained from Tamada and examined at NRL showed optimum effects only in localized small areas of his films. The Bi containing films are co-doped with Lu in place of Y in order to obtain high Faraday rotations with substantial lattice matching to GGG substrates.

2.0 Experimental

2.1 Film Growth

Films of $Bi_{3-X}Lu_XFe_5O_{12}$ single crystal garnet with X = 2.17 were grown by the horizontal dipping method of liquid phase epitaxy. One inch diameter substrates of GGG were used. These were grown and polished to standard ASTM/SEMI specifications on both sides of the wafer. Films were grown singly using the composition described by Tamada.(4) This composition is unique in that only Bi_2O_3 is used as a solvent and no incorporation of Pb can occur. The latter can cause increased optical absorption and FMR linewidth. Fluxed melts are usually described by various ratios of their constituents. Thus in our melts we define

$$R1 = Fe_2O_3/Lu_2O_3 = 7.73$$

$$R_4 = (Fe_2O_3+Lu_2O_3)/Fe_2O_3+Lu_2O_3 + Bi_2O_3 = 0.17$$

$$R16 = MgO/(2Fe_2O_3+MgO) = 0.000 \text{ to } 0.47$$

Films were grown from 2 inch diameter x 2 inch high cylindrical crucibles fabricated from platinum. Some films were also grown in very low gradient melts contained in 4 inch diameter x 6 inch high crucibles.

All of the chemicals used in formulating our melts, Bi_2O_3, Fe_2O_3, Lu_2O_3, and MgO were 99.99% purity or better. The Bi_2O_3 was free of lead and the Lu_2O_3 was devoid of any other rare earths which may cause significant broadening of the film's FMR linewidth (ΔH). The general procedures and equipment for film growth were explained more fully in a previous reference.(6) Our films were grown at a temperature of 814-817°C with special emphasis on attaining a near X-ray lattice constant match between the film and the GGG substrate. The substrate rotation rate was 100 rpm during growth with a rotation reversal rate of five seconds. Growth rates were rather slow at 0.4-0.6 μm/minute in order to obtain high film quality. The film thickness was controlled in the range of 1-10 μm. A few special films were grown under conditions which were unique for growth rate, melt temperature, or drift in melt temperature with time. These were chosen in order to (1) Minimize the appearance of any compositional

transition layer between substrate and film. (2) Minimize the appearance of the $LuFeO_3$ or $BiFeO_3$ orthoferrite phases which may introduce defects and cause broadening of ΔH. (3) Obtaining nearly exact lattice constant matches to prevent high strain or cracking in the films.

2.2 Measurements

Several measurements were made on film properties to control growth reproducibility and device response. Most of these techniques were developed earlier during the course of magnetic bubble memory research. A good survey on standard methods has been recorded by Josephs.(7)

The film thickness was measured by an optical interference fringe technique. The uniformity of thickness was also observed over the entire area of the one inch diameter film. It should be noted that film thickness can also be estimated by direct weighing of the sample before and after growth. A knowledge of the amount of material removed from the melt is helpful to replace the exact weight of components and return to the same initial composition. The index of refraction of the composition is needed for accurate thin film analysis. This value was estimated from other bismuth garnets of the equivalent compositions. Little error is made in this approximation.

The X-ray lattice constants of the film relative to the GGG substrate were measured on a diffractometer by using reflections from (888) high angle planes. All of the substrates possessed the same lattice constant as indicated by reproducible 2θ angles. The films' lattice constant could be calculated by measuring peak differences due to the $K\alpha$, lines and their separation. Both substrate and film could be recorded on the same diffractometer trace because of the μm film thickness. Films were grown lattice matched, in tension or in compression depending on the films' cell constant, a_f, compared to the substrate, a_s.

Another important film parameter is the mean growth rate which is defined by the film thickness divided by the total growth time.

Defect densities were determined by microscopic examination over the entire area of a film. Visible defects to a resolution of about 1 μ are counted. These included dislocations propagated from the substrate, bubbles, inclusions of platinum, bismuth, or orthoferrites, "footprints" from flux residues, particles, or other phases imbedded in the film surface, and scratch damage.

Optical absorption of the samples was measured with a Cary Model 17 Spectrophotometer. Some samples were also checked on a Nicolet Model 20-DXB FT infrared spectrometer.

The Faraday rotation was measured by a nulling method which employed a laser source, polarizer, analyzer, and suitable detectors. Our apparatus was constructed by Optics for Research of Caldwell, NJ. The samples were placed in sufficient magnetic fields to saturate the magnetization.

Resistance measurements were performed by a four point probe technique.

The ferromagnetic resonance linewidth, ΔH, was determined at 9.1 GHz by means of a non resonant method consisting of a short circuited waveguide. This is generally suitable for a large signal and small ΔH. The methods developed by Takeda (8) and Adam (11) were particularly applicable since they can be non destructive on small areas of large wafers. Furthermore they are quite sensitive to the presence of defects in the films.

Passband measurements were performed on our films with equipment at University of Delaware and Westinghouse Research. These measurements are essentially loss as a function of frequency where the former is measured by appropriate transducers spaced from the film. The film is under an applied perpendicular bias field of 2-4 kG where a forward volume wave is utilized. The film is acting as a single channel element with the measured loss due only to the material. Comparisons can be made readily to low linewidth pure YIG films.

3.0 Results and Discussion

3.1 Films with Low Optical Absorption

The first film growth approach was to duplicate the work of Tamada, et. al [4] who reported the growth of $(BiLu)_3Fe_5O_5$ films with low optical absorption (< 1 db/cm) and low ferromagnetic resonance linewidth (< 1 Oe). They controlled the optical absorption by small amounts of MgO expressed as a R^16 ratio equal to [MgO/(2 Fe_2O_3 + MgO)] X 100. The Mg^{2+} ions compensates the charge of the Pt^{4+} ions that are introduced due to growth in platinum crucibles. Otherwise Fe^{2+} ions are formed which broaden the linewidth.

When efforts were made to reproduce Tamada's work using melt 1 tabulated in Table 1 it was found that the solidified flux damaged the films upon removing them from the furnace. As seen in Figure 1 the Bi_2O_3 flux partially wets the magneto-optic film. After removing the flux with acetic acid the film shows a damaged area where the flux used to be (Fig 2). A 200X reflected light optical examination seen in Fig 3 of the edge of the damaged area shows damage to the film caused by the solidifying flux. An examination of the damaged area by scanning electron microscopy (Fig 4) shows that 10-30μm size pieces of the film are ripped off the substrate. To circumvent this problem a series of films were grown (films AA-54 through AA-69 in Table 2) using different techniques to encourage the draining of the flux prior to pulling the film out of the furnace and solidifying the flux. Using substrate tilt angles up to 12^o and holding the post-grown film above the melt shortly after growth to drain the flux off was moderately successful. Figure 5 is a 1X photograph of a film grown out of a $R'6 = 0$ melt using a 12^o tilt on the holder. The residual flux droplets tend to be located near the edges of the film. When the $R'6$ coefficient is raised to 1% by adding MgO to the melt the flux becomes substantially more non-wetting and the flux removal problem was lessened. Figure 6 is a photograph of a film grown from a $R'6 = 1\%$ melt using the same technique as the film in fig 4. It can be seen that the flux removal is more complete. Since the film was damaged under the residual flux droplets a substantial portion of the film is usable.

Table 1. Melt and growth conditions for the Bi_2O_3 fluxed growth of $(BiLu)_3Fe_5O_{12}$ films to duplicate the work of Tamada, et. al.(4)

	Amount in grams					
Chemical	**Melt 1**	**Melt 2**	**Melt 3**	**Melt 4**	**Melt 5**	**Melt 6**
Bi_2O_3- 99.999%	466.0	466.0	466.0	466.0	466.0	466.0
Fe_2O_3 - 99.99%	28.9	28.9	28.9	28.9	28.9	2.9
Lu_2O_3 - 99.99%	9.6	9.6	9.6	9.6	9.6	9.6
MgO - 99.99%	0.0	0.15	0.23	0.30	0.39	0.47
$R6^1$ in mole %	0	0.15	0.23	0.30	0.39	0.47
Growth temperature to lattice match film to substrate	814	815	815	816	817	817
Substrate rotation rate during growth rpm/ reversal time in seconds	100/5	100/5	100/5	100/5	100/5	100/5
Growth rate μm/min.	0.66	0.58	0.44	0.42	0.40	0.38

Figure 1. 1.3X photograph of magneto-optic film with partially wetting Bi_2O_3 solidified flux mound.

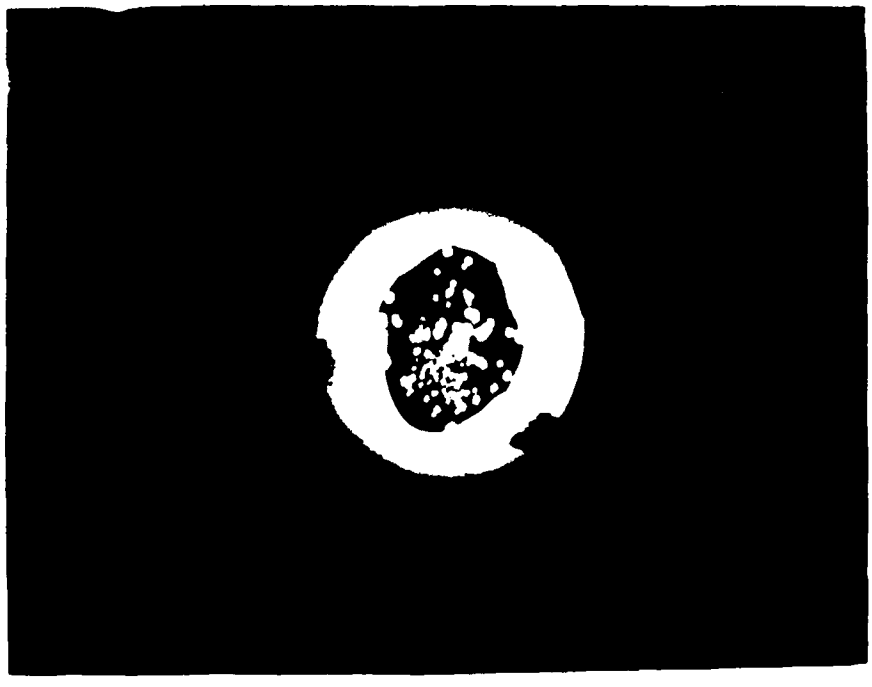

Figure 2. 1.3X photograph of magneto-optic film after the Bi_2O_3 flux has been removed by acetic acid.

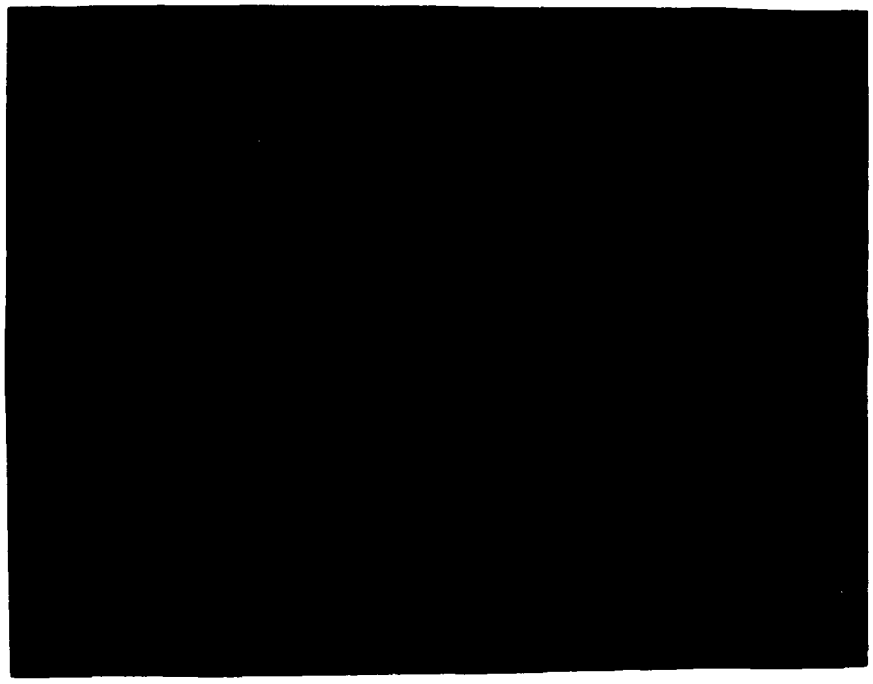

Figure 3. 200X reflected light micrograph of area under flux mound showing damage to the magneto-optic film. The undamaged film is in the upper right hand corner of the micrograph.

Figure 4. A 1000X secondary electron micrograph of the surface of a magneto-optic film showing pieces of the film ripped off the substrate when the Bi_2O_3 flux solidifies.

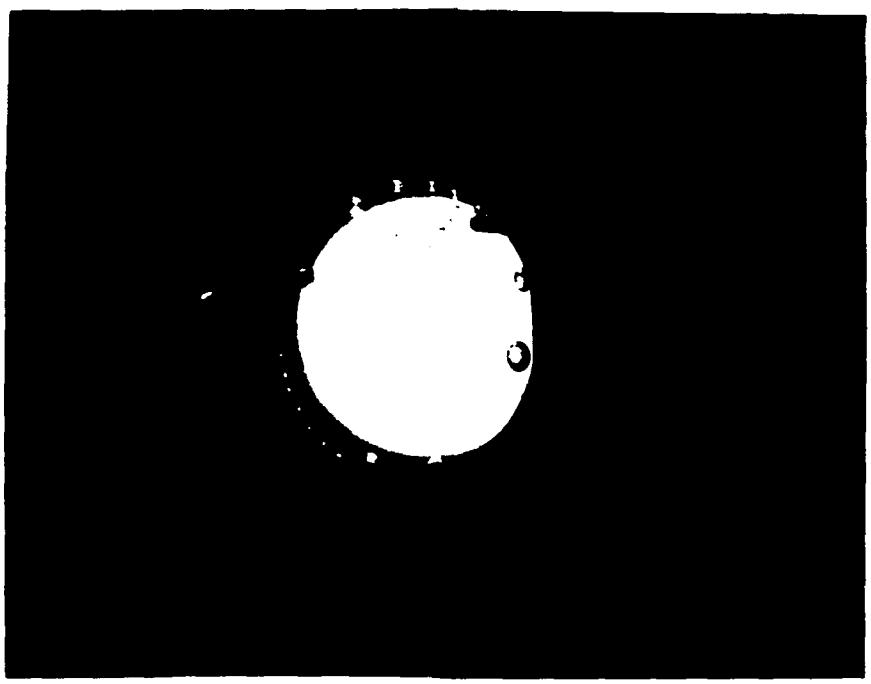

Figure 5. 1X photograph of a magneto-optic film showing residual flux droplets. The film was grown from a Bi_2O_3 flux with a R6 = 0 using a 12^o tilt on the substrate and 800 rpm spin off to facilitate flux removal.

Table 2. Summary of Growth and Physical Properties of $(BiLu)_3Fe_5O_{12}$ Films

Film	Melt No.	R'6%	Thickness μm	Lattice Constant Mismatch A	Growth Rate μm/min	Melt Temperature °C	Drift in Melt Temp ± °C	Growth Time min.
AA-48	1	0	4.2	0.012C	0.84	795	0.5	5
AA-50	1	0	6.3	0.023C	1.26	798	4.0	5
AA-52	1	0	3.4	0.000	0.68	815	2.0	5
AA-54	1	0	9.5	0.000	0.67	816	1.5	14
AA-57	1	0	10.4	0.003	0.74	812	2.0	14
AA-59	1	0	10.7	0.006C	0.76	810	1.0	14
AA-61	1	0	9.5	0.004C	0.68	813	0.3	14
AA-63	1	0	6.6	0.011C	0.47	820	0.8	14
AA-68	1	0	9.7	0.004C	0.69	813	2.0	14
AA-69	1	0	4.4	0.001T	0.63	814	0.3	7
AA-71	2	1	8.2	0.003C	0.59	815	1.0	14
AA-74	3	1.5	6.1	0.003T	0.44	817	0.6	14
AA-76	3	1.5	3.2	0.002T	0.46	818	0.5	7
AA-78	4	2	7.4	0.000	0.53	815	0.3	14
AA-80	4	2	6.1			815	0.3	7
AA-81	4	2	3.6			813	0.4	12
AA-82	5	2.7	2.6	0.000	0.36	816	0.4	7
AA-83	5	2.7	5.1	0.000	0.36	816	0.2	14
AA-84	5	2.7	3.7	0.010C	0.53	815	0.4	7
AA-86	5	2.7	2.9	0.003T	0.41	817	0.4	7
AA-91	6	3.1	4.0		0.40	816	0.5	10
AA-96	6	3.1	6.9			817	0.5	20
AA-120	7	1.1	1.8	0.060C	0.30	774	0.1	6
AA-122	7	1.1	7.5	0.004T	0.75	728	0.4	10
AA-124	7	1.1	6.1	0.002C	0.76	723	0.4	8

Film	Melt No.	R'6%	Thickness μm	Lattice Constant Mismatch A	Growth Rate μm/min	Melt Temperature °C	Drift in Melt Temp ± °C	Growth Time min.
AA-128	7	1.1	6.1	0.000	0.76	726	0.5	8
AA-133	8	1.1	2.0	0.049T	0.25	718	1.0	8
AA-135	8	1.1	1.0	0.029T	0.13	712	1.0	8
AA-137	8	1.1	1.5	0.001T	0.19	696	1.0	8
AA-139	8	1.1	5.9	0.006C	0.18	693	1.0	32
AA-142	8	1.1	5.6	0.000	0.18	692	2.0	32
AA-144	8	1.1	5.4	0.003T	0.17	693	1.5	32
DD-5	9	1.1	10.3	0.017C	0.3	689	1.8	32
DD-8	9	1.1	9.6	0.017C	0.3	689	3.1	32
DD-10	9	1.1	9.5	0.014C	0.3	690	0.4	32
DD-12	9	1.1	8.5	0.013C	0.3	691	0.2	32
DD-14	9	1.1	6.7	0.008T	0.23	702	0.7	32
DD-17	9	1.1	5.8	0.002T	0.23	700	0.1	25
DD-20	9	1.1	6.7	0.002T	0.23	699	0.2	28
DD-22	9	1.1	6.6	0.002T	0.23	697	0.4	28
DD-25	9	1.1	8.3	0.006C	0.33	691	1.3	28
DD-27	9	1.1	6.6	0.000	0.23	696	0.1	28
DD-29	9	1.1	4.4	0.006C	0.22	693	0.5	20
DD-30	9	1.1	5.9	0.003C	0.24	694	0.7	25
DD-32	9	1.1	5.7	0.002C	0.23	695	0.2	25
DD-33	9	1.1	5.9	0.006C	0.24	693	0.7	25
DD-34	9	1.1	5.7	0.000	0.23	697	1.4	25
DD-35	9	1.1	5.7	0.002C	0.23	694	1.8	25
DD-37	9	1.1	5.4	0.005C	0.22	695	0.5	25
DD-41	9	1.1	5.7	0.006C	0.23	694	0.4	25
DD-43	9	1.1	5.6	0.002C	0.22	693	0.5	25

Film	Melt No.	R'6%	Thickness μm	Lattice Constant Mismatch A	Growth Rate μm/min	Melt Temperature °C	Drift in Melt Temp ± °C	Growth Time min.
DD-45	9	1.1	6.5	0.008C	0.26	693	0.6	25
DD-47	9	1.1	5.3	0.000	0.21	693	0.6	25
DD-49	9	1.1	5.1	0.002C	0.20	694	0.5	25
DD-51	9	1.1	5.2	0.009C	0.21	695	0.5	25
DD-81	10	1.1	1.8	0.047T	0.06	722	1.4	30
DD-83	10	1.1	1.0	0.008C	0.03	684	1.4	30
DD-84	10	1.1	1.0	0.090T	0.03	733	1.4	30
DD-87	10	1.1	4.0	0.020T	0.13	702	1.5	30
DD-91	10	1.1	4.9	0.009T	0.11	702	2.3	45
DD-93	10	1.1	8.2	0.010T	0.15	697	4.0	55
DD-97	9	1.1	5.1	0.008C	0.20	686	7.0	25
DD-99	9	1.1	3.9	0.018T	0.14	702	0.1	28
DD-102	9	1.1	5.5	0.000	0.19	691	0.3	30
DD-104	9	1.1	6.2	0.000	0.21	691	0.3	30
DD-105	9	1.1	5.4	0.000	0.18	690	0.1	30
DD-107	9	1.1	-	-	-	691	0.5	30
DD-109	9	1.1	5.3	0.000	0.18	690	0.05	30
DD-111	9	1.1	5.1	0.000	0.17	692	0.1	30
DD-114	9	1.1	5.1	0.000	0.17	692	0.3	30
DD-117	9	1.1	5.4	0.000	0.18	691	0.1	30
DD-124	9	1.1	4.8	0.000	0.16	692	0.5	30
DD-126	9	1.1	4.6	0.000	0.15	692	0.1	30
DD-128	9	1.1	4.6	0.000	0.15	691	0.1	30
DD-129	9	1.1	4.4	0.000	0.15	693	0.1	30
DD-130	11	1.1	13.7	0.016T	0.11	691	0.8	120
DD-133	11	1.1	10.0	0.014T	0.11	691	1.0	88

Film	Melt No.	R'6%	Thickness μm	Lattice Constant Mismatch A	Growth Rate μm/min	Melt Temperature °C	Drift in Melt Temp ± °C	Growth Time min.
DD-138	12	1.1	5.8	0.035T	0.06	691	0.8	96
DD-140	13	1.1	4.5	0.000	0.19	692	1.0	24
DD-142	9	1.1	6.4	0.007T	0.21	672	1.5	30
DD-143	9	1.1	7.2	0.006C	0.24	692	0.3	30
DD-151	14	0.0	8.3	0.030C	-	806	0.5	12
KK-5	14	0.0	8.4	0.002T	0.70	814	0.5	12
KK-6	14	0.0	8.4	0.002T	0.70	814	0.5	12
KK-7	14	0.0	8.4	0.002T	0.70	814	0.5	12
KK-8	14	0.0	8.3	0.003T	0.69	815	0.4	12
KK-9	14	0.0	9.5	0.008C	1.0	812	1.1	9
KK-10	14	0.0	9.5	0.008C	1.1	812	0.5	9
KK-12	14	0.0	3.5	0.003T	0.7	815	0.5	5
KK-13	14	0.0	4.3	0.003T	0.70	815	0.5	6
KK-16	14	0.0	4.5	0.002C	0.56	814	0.5	8
KK-18	14	0.0	4.5	0.002C	0.56	813	0.5	8
KK-19	14	0.0	4.8	0.000	0.60	815	0.5	8
KK-20	14	0.0	4.8	0.000	0.60	815	0.5	8
KK-23	14	0.0	8.8	0.011C	1.1	814	0.5	8
KK-24	14	0.0	7.9	0.016C	1.0	813	0.5	8
KK-25	14	0.0	-	0.010C	-	814	0.5	8
KK-26	14	0.0	4.5	0.002	0.56	812	0.5	8
KK-27	14	0.0	4.4	0.002C	0.55	813	0.5	8
KK-36	8	1.1	5.8	0.070C	0.83	755	0.2	7
KK-37	8	1.1	6.0	0.005C	0.85	770	0.2	7
KK-38	8	1.1	2.7	0.076C	0.85	755	0.1	2
KK-42	8	1.1	-	0.054C	-	785	0.1	2

Film	Melt No.	R'6%	Thickness μm	Lattice Constant Mismatch A	Growth Rate μm/min	Melt Temperature °C	Drift in Melt Temp ± °C	Growth Time min.
KK-43	8	1.1	1.0	0.085C	0.5	791	0.1	2
KK-44	8	1.1	1.0	0.072C	0.5	813	0.1	2
KK-45	8	1.1	0.8	0.064C	0.4	822	0.1	2
KK-46	8	1.1	0.9	0.030	0.2	822	0.2	4.5
KK-47	8	1.1	1.6	0.060C	0.2	822	0.4	8
KK-49	8	1.1	1.0	0.054C	0.1	828	0.5	9.5
KK-50	8	1.1	0.5	-	0.03	839	1.0	17

Furthermore increasing the MgO content of the melt up to R'6 = 3.1% did not substantially affect the flux removal. Once the problem of flux removal was circumvented a series of films were grown using increasing amounts of MgO in the melt (9 films AA-71 through AA-96 in Table 2). For each R'6 composition at least one thin, circa 3μm, and one thick circa 7μm film was grown to determine the coefficient of optical absorption at 1300nm using the method of Takeuchi, et. al..[9] The thin film was also prepared for ferromagnetic resonance linewidth measurements by polishing off the back side film and cutting the film into 1x2mm pieces with a precision diamond dicing saw. The FMR linewidth was measured at 9.1 GHz by insertion into a terminated waveguide. The FMR samples were then annealed at 800°C for four hours in flowing oxygen and then the linewidths were remeasured to study the possible affect of oxygen vacancies on FMR linewidths. Later Tamada, et. al., [10] would report a modest lowering of FMR linewidths with the same composition upon annealing in an ozone atmosphere.

3.2 Flux Problems

A second film growth approach was undertaken to try to correct the problem with surface damage to the film by the adhering flux. J.D. Adam, et. al.,[11] reported surface roughness or damage degraded the microwave pass bands in YIG films which prompted the consideration of a Bi_2O_3-Na_2O flux which was known not to damage magneto-optic film surfaces.[6] A series of films were grown (films AA-120 through AA-128, Table 2) to adjust the melt temperature to lattice match the film to the substrate. The melt used is identified as melt 7 in Table 3. It was noted that the Tamada formulation resulted in the precipitation of the $LuFeO_3$ orthoferrite phase along with the garnet phase. A series of films were grown (AA-133 through AA-144 in Table 2) to adjust the R1 value from the Tamada value of 7.5 to an R1 value of 12 which did not precipitate the orthoferrite phase. The R'6 value of this melt was 1.1% which is the minimum in optical absorption at 1300nm. This melt, melt 8, is also given in Table 3. Once the melt composition and

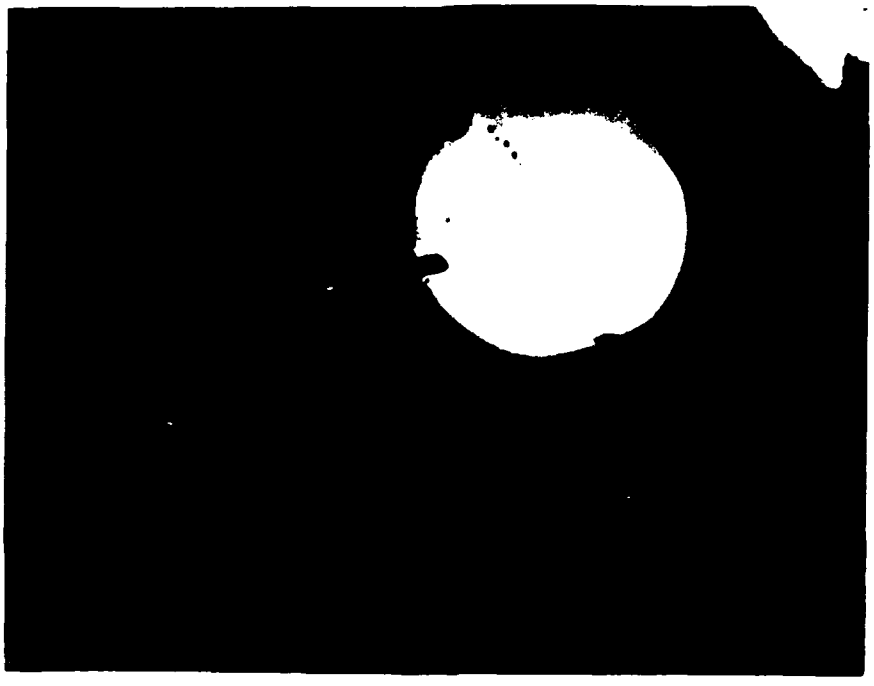

Figure 6. 1.5X photograph of film grown from a R6 = 1% melt using the same growth technique as in figure 4. The increase in MgO content of the melt has lessened the problem of flux removal by making the flux more non-wettable, and therefore easier to remove from the film surface by rapid spinning.

growth parameters were established a series of films circa 5μm thick and nearly lattice matched were grown for pass band measurements at NRL and Westinghouse. A special effort was made to keep the growth rate constant by keeping the growth temperature as constant as possible during growth. In addition efforts were made to grow nearly defect free films as growth defects were known to affect FMR linewidth.(9) For this series of films a new melt was utilized identical to melt 8 except when the melt was being formulated oxygen was blown into the melt via a platinum tube. It was believed this could reduce some of the Pt^{4+} uptake in the film. All Bi_2O_3 based melts attack the platinum crucibles to a certain extent. Films DD-5 through DD-51 in Table 2 were grown for these passband measurements. Of these films five films listed in Table 4 were growth and substrate defect-free. These films were grown under carefully controlled conditions such that the melt temperature did not drift more than 0.9°C over a 25 minute long growth run. Every cm^2 of each of these films were examined under 200X optical microscope and were determined to be entirely defect-free. These were put forth as the best films to be examined for passband measurements.

3.3 Growth Rate Modifications

The third approach to the film growth was selected when the passband measurements on some of the best films grown to date turned out to have poor passbands. A decision was made to grow the films as rapidly as possible and as slow as possible with the understanding that the film to substrate lattice mismatch would suffer. The approach was selected due to the belief the transition layer, known to exist in magnetic films grown by the liquid phase epitaxy method, could be causing spin wave coupling which deteriorates the passband.(11) A decision was made to grow both rapidly and slowly to vary the width of the transition layer. It was hoped some insight could be gleaned from the effect of growth rate on the passband.

The next series of films (films DD-81 through DD-93 in Table 2) were grown from melt 10 listed in Table 3. The goal was to grow slowly. A rotation rate of 5-10

Table 3. Melt and growth conditions for the Bi_2O_3-Na_2O fluxed growth of $(BiLu)_3Fe_5O_{12}$films. The addition of Na_2O to the flux was used to avoid the flux damage to the film with the Tamada growth method.

	Amount in grams							
Chemical	**Melt 7**	**Melt 8**	**Melt 9**	**Melt 10**	**Melt 11**	**Melt 12**	**Melt 13**	**Melt 14**
Bi_2O_3 - 99.999%	466.0	745.0	745.0	745.0	745.0	745.0	745.0	2330.0
Na_2CO_3 - 99.999%	32.0	51.6	51.6	51.6	51.6	51.6	51.6	0.0
Fe_2O_3 - 99.999%	28.9	46.1	46.1	46.1	46.1	46.1	46.1	144.4
Lu_2O_3 - 99.999%	9.6	9.6	9.6	9.6	9.6	9.6	9.6	47.8
MgO - 099.999%	0.26	0.26	0.26	0.26	0.26	0.26	0.26	0.0
R^16 in mole %	1.1	1.1	1.1	1.1	1.1	1.1	1.1	0.0
Growth temperature to lattice match film to substrate	726	692	692	691	n/a	n/a	n/a	85
Substrate rotation rate during growth rpm/reversal time in sec.	100/5	100/5	100/5	50/10	25/00	10/00	300/5	100/5
Growth rate μm/min.	0.76	0.18	0.18	0.09	0.11	0.06	0.19	0.80
Melt oxygenated during melt preparation?	No	No	Yes	Yes	Yes	Yes	Yes	No

Table 4. Growth and film properties of essentially defect-free magneto-optic films grown for passband measurements.

Film	Thickness μm	Lattice Mismatch A	Total Defects per film	Defect Type	Temperature drift	Growth Rate μm/mm
DD-37	5.4	0.005C	0	-	0.4	0.22
DD-41	5.4	0.006C	2	Subsurface damage	0.8	0.22
DD-43	5.6	0.002C	0	-	0.9	0.22
DD-47	5.3	0.000C	0		0.4	0.21
DD-49	5.1	0.002C	0	-	0.9	0.20

rpm was used. This was suggested by H. Huahuri, et. al.,[12] who prepared $Lu_{2.15}Bi_{0.85}Fe_5O_{12}$ films with a reported FMR linewidth of 0.5 Oe and a bandwidth of 400MHz at a frequency of 4.0 GHz. The last films in this series, grown between 0.11 and 0.15μm/min., were very much in tension and cracked due to the lattice mismatch stress. In films DD-130 and DD-133 the rotation rate was lowered to 25 rpm with no reversal to further flow down the growth rate. These films grew at 0.11μm/min. Film DD-130 had only a total of 18 defects per total film area (3.5 defects/cm^2) and is an excellent film to test the hypothesis of slow growth. Film DD-133 broke in two equal pieces. Film DD-138 was grown at a rotation rate of 10 rpm with no reversal to further slow down the growth rate. It grew at 0.06μm/min. but the film was badly cracked due to the tensile stress. In films DD-140 through DD-143 an effort was made to rapidly grow the films. This effort was not successful due to the age of the melt. A significant amount of platinum precipitate had formed on the bottom of the melt causing the melt prematurely to nucleate. The melt was then dumped.

3.4 Film Quality and Defect Study

The fourth film growth approach was to go back to Tamada's [4] original work and grow the best quality Na_2O and MgO - free films possible. The films from DD-151 through KK-27 in Table 2 were grown using this approach. The problem encountered early in this study with the flux damage using the Bi_2O_3 melt resurfaced. A larger 1.5 kg melt was used in a larger epitaxial furnace to add more flexibility in the film growth. Several tilt angles were used. In the first study films AA-54 through AA-69 in Table 2 used a 12^o tilt angle to facilitate flux drainage. Here 45^o and 90^o tilt angles were employed using specially designed holders which could only be used in a larger furnace. The approach met with only marginal success. Most of the films either cracked or suffered substantial damage to the film surface, often so bad as to make film thickness measurements by the optical interference method impossible. A few films, however, such as KK-24 and KK-27 were useful for passband measurements.

The fifth growth approach was to grow circa 1.8μm thick films with as much Bi substitution as possible. In this scheme the magneto-optic film would only be used to carry the optical signal. The magnetostatic wave would be propagated in a separate YIG film held in close proximity. A series of films were grown from a Bi_2O_3-Na_2O melt and a R'6 value of 1.1. This composition was selected, as it gave a minimum in optical absorbance at 1300nm and good film quality. Films KK-36 through KK-50 in Table 2 were grown in this series. Since the film thickness was small, substantially more Bi_2O_3 could be forced into the film before the film quality degraded. Films KK-37, KK-38, KK-44, KK-45, KK-46 and KK-47 are candidates for use in devices. Some of these films have a surface roughness associated with excessive lattice strain but can be polished flat for device work.

The sixth growth approach involved the intentional introduction of defects into the magneto-optic films. Experience with growing YIG films has shown that large numbers of defects are needed before there is a moderate effect on FMR linewidth.(11) It was of interest to investigate the possible role of a range of sizes of growth induced defects had on the linewidth and passband. Various methods are possible for the controlled introduction of defects into magneto-optic films.(13) Defects were introduced into a series of films (DD-97 through DD-143 in Table 2) by forcefully blowing a spray of carefully sized diamond grit against a substrate prior to growth. Diamond sizes of 1/4, 1, 3, 9, and 30μm were employed to introduce a range of sizes of subsurface damages in the substrates. Upon subsequent growth the subsurface damage in the substrate results in growth dislocations in the film. The size of the defects were documented and the film sent out for passband measurements.

The first series of films grown using the Bi_2O_3 flux was duplicated from the work of Tamada, et. al..(4) In Table 5 it can be seen that the minimum in optical absorption occurs at different R^16 values depending on the wavelength. For a wavelength of 1152nm, the wavelength used by Tamada, the minimum in optical

absorption occurs at an R^16 value of 2.0. This is in agreement with Tamada who also reported a minimum in optical absorption at 1152nm at an R^16 value of 2.0. For 1300nm the present study finds a minimum in optical absorption between an R^16 value of 1 and 1.5%.

It was also noted that as the R^16 value was increased from $R^16 = 0$ to 3.1. The growth rate dropped from 0.66 to 0.38μm/min. under similar supercoolings. This was similar to that reported by Roode and Robertson (15) who did the early work in the area of growth inhibitors for bubble memory films.

The FMR linewidths of the films grown with the various R^16 values are given in Table 6, for both the as grown state and annealed in O_2 for four hours at 800°C. No apparent trend could be seen from the data connecting the R^16 value with the FMR linewidth. A comparison of these values to Tamada's data (Table 6) shows the linewidth values in this study were higher than Tamada's values even though the film growth parameters were apparently similar. The samples in Table 5 were sent to NRL for passband measurements.

The series of films grown from the Bi_2O_3-Na_2O flux did not suffer the damage to the film surface that the film did from the straight Bi_2O_3 flux. The Bi_2O_3 flux upon cooling ripped off small pieces of the film (circa 10μm) off the substrate. The same was true of the Bi_2O_2-Na_2O flux if the flux was not adequately spun off. If a thick layer of flux remained when the flux cooled it also damaged the film. The Bi_2O_3-Na_2O flux, because of its wetting nature, can easily spin off so as to leave only a thin layer of flux. This flux, upon cooling, tends to spall off the film surface without damaging the film. Of all the films grown from the Bi_2O_3-Na_2O flux, five films in Table 7 were hand picked to be best and were sent to NRL in May, 1990 for FMR passband measurement. The entire area of these films were examined under a 200X optical microscope and were found to be absolutely free of defects above 0.5 to 1μm in size. Film DD-41 had two defects related to minor subsurface damage in the substrate. The temperature drift during

Table 5. Effect of R^16 value on the optical absorption and growth rate of $(BiLu)_3Fe_5O_{12}$ films.

Sample	Mole % MgO in Melt	Total 2 Sided Thickness in μm	α cm^{-1} at 1300nm	α cm^{-1} at 1152nm	Growth Rate (μm/m)
AA-61	0	18.4	121	133	0.66
AA-69	0	8.8	121	133	0.66
AA-71	1	15.3	0	58	0.58
AA-71 Etched	1	6.5	0	58	0.58
AA-74	1.5	11.8	0	43	0.44
AA-76	1.5	6.4	0	43	0.44
AA-78	2	14.7	170	0	0.51
AA-81	2	7.1	170	0	0.51
AA-83	2.7	10.6	93	390	0.40
AA-86	2.7	5.7	93	390	0.40
AA-91	3.1	7.6	148	202	0.38
AA-96	3.1	13.8	148	202	0.38

Table 6. Comparison of the ferromagnetic linewidth of films grown in this study and by Tamada.[16] Both were grown under apparently the same conditions.

R16 Value	Airtron As grown	Airtron O_2 annealed - 4hr 800ºC	Tamada (Ref. C)
0	1.5	2.5	1.7
1	3.0	3.0	1.0
1.5	-	-	0.9
2	2.8	2.5	0.8 interpolated
2.7	3.3	3.0	0.8

minute run was held to $\pm$ 0.5°C. These films represented the best of the films grown during this study. The passbands of two of these films (DD-43 and DD-49) were measured at Westinghouse and, as can be seen in Figures 7 and 8, were extremely poor. The top trace was the return loss and the bottom trace was the insertion loss. A passband trace of a YIG film that worked well in a MSW device is given in Figure 9 for comparison. It was clear that the $(BiLu)_3Fe_5O_{12}$ films grown by the best techniques in this study had poor passbands. Of all the passbands measured only three films stand out as having any insertion loss. These films were DD-10, DD-25, and DD-33. Of these films only DD-33 (Figures 10 and 11) improved after etching off 0.3μm of the film surface. Another film (DD-49) did not improve upon etching off 0.1μm. The before and after etching passbands can be seen in Figures 12 and 13. Film DD-10 (Figure 14) did improve slightly upon annealing for 72 hours in O_2 at 850°C but many others did not. Of the three films mentioned the substrate lattice mismatch varied from 0.002 A in tension to 0.014 A in compression. Clearly an even larger variation in lattice mismatch does not affect the passband measurements. In addition the five films selected as having absolutely zero defects and grown under the best melt temperature drift conditions had some of the worst passbands. Clearly the traditionally controlled film growth properties as lattice mismatch, defect density, linewidth, and lattice constant variation within the film thickness do not significantly affect the MSW passband. The linewidths measured nondestructively on these films using the method of Adam, et. al., [17] were in the range acceptable for YIG MSW devices. The FMR linewidth of a typical film grown from the Bi_2O_3-Na_2O flux (film AA-144) was 1.5 and 0.7 Oe depending on the resonance measured. The FMR spectra for this film is given in Figures 15, 16, and 17. Figure 15 is the spectrum taken from 5250 to 5750 Oe showing all the resonance. Figures 16 and 17 are close up traces of the resonances labeled 1 and 2 in Figure 15.

It is interesting to speculate on why bismuth containing films have bad passbands while YIG films can have very good passbands. It may be due to the intrinsic nature of

Table 7. Five of the best $(BiLu)_3Fe_5O_{12}$ films grown in this study from the Bi_2O_3-Na_2O flux.

Film	Thickness μm	Lattice Mismatch A	Total Defects per film	Defect Type	Temperature drift	Growth Rate μm/mm
DD-37	5.4	0.005C	0	-	0.4	0.22
DD-41	5.4	0.006C	2	Subsurface damage	0.8	0.22
DD-43	5.6	0.002C	0	-	0.9	0.22
DD-47	5.3	0.000C	0		0.4	0.21
DD-49	5.1	0.002C	0	-	0.9	0.20

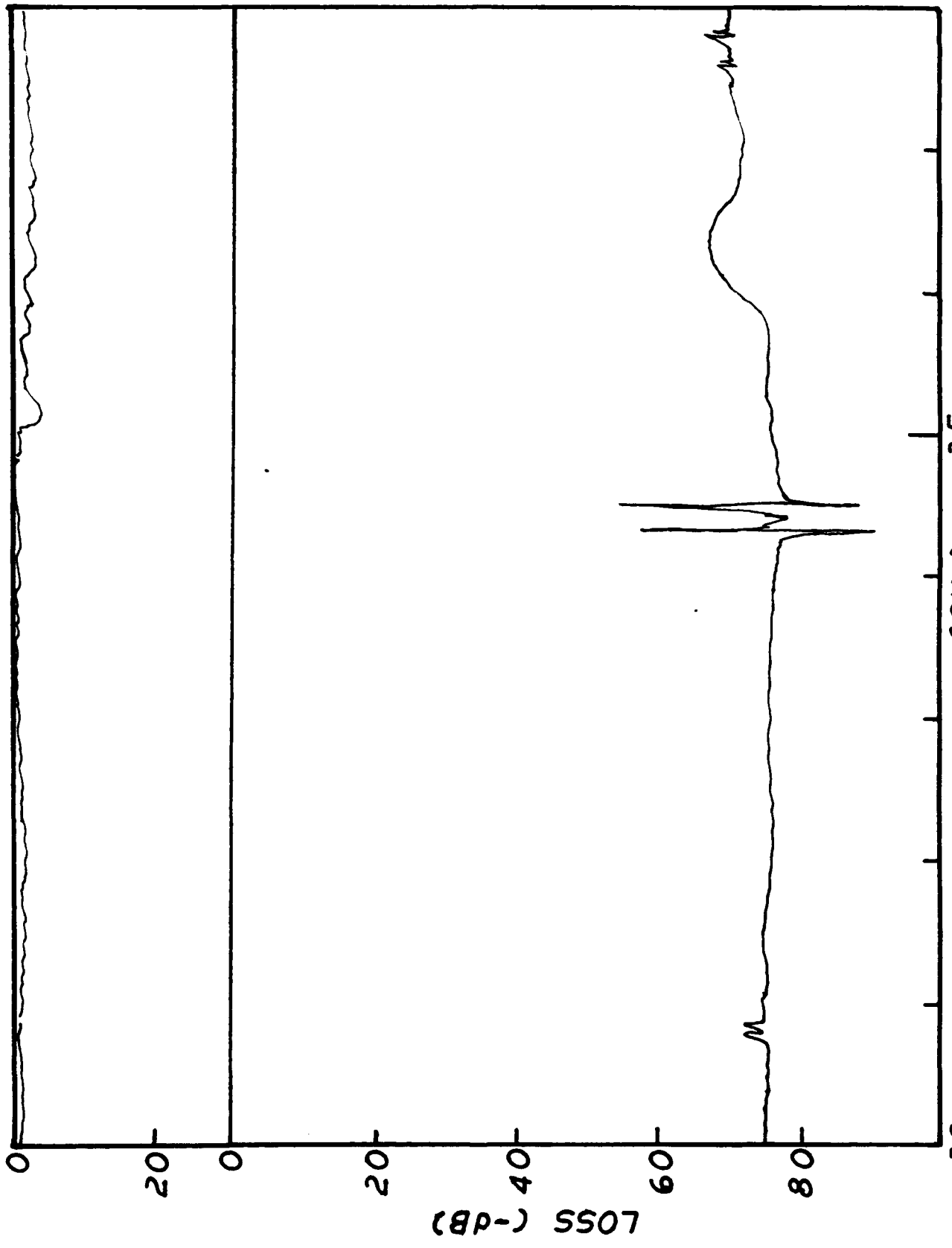

Fig. 7 MSW measurements on $(BiLu)_3Fe_5O_{12}$ film DD43.

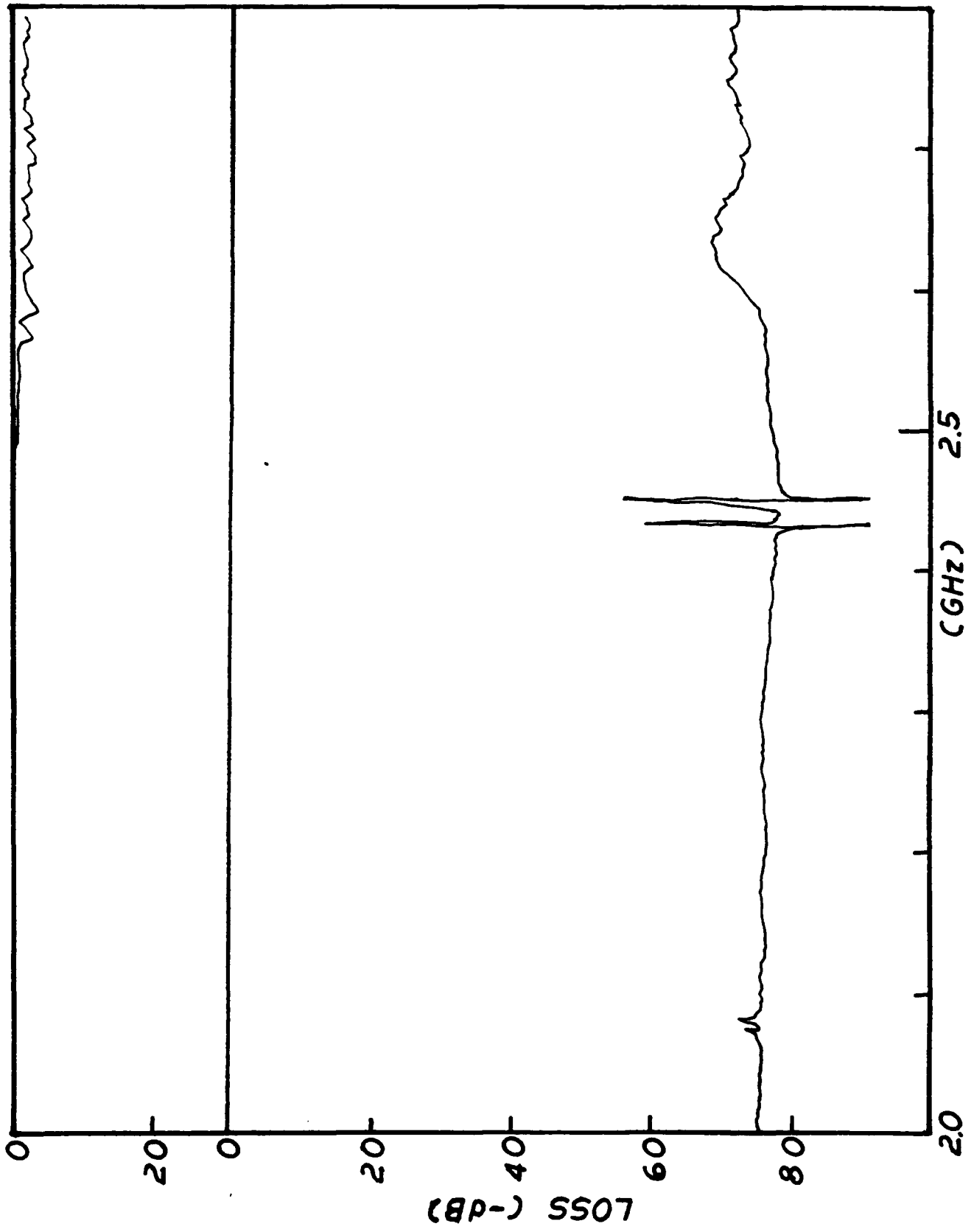

Fig. 8 MSW measurements made on Film DD-49.

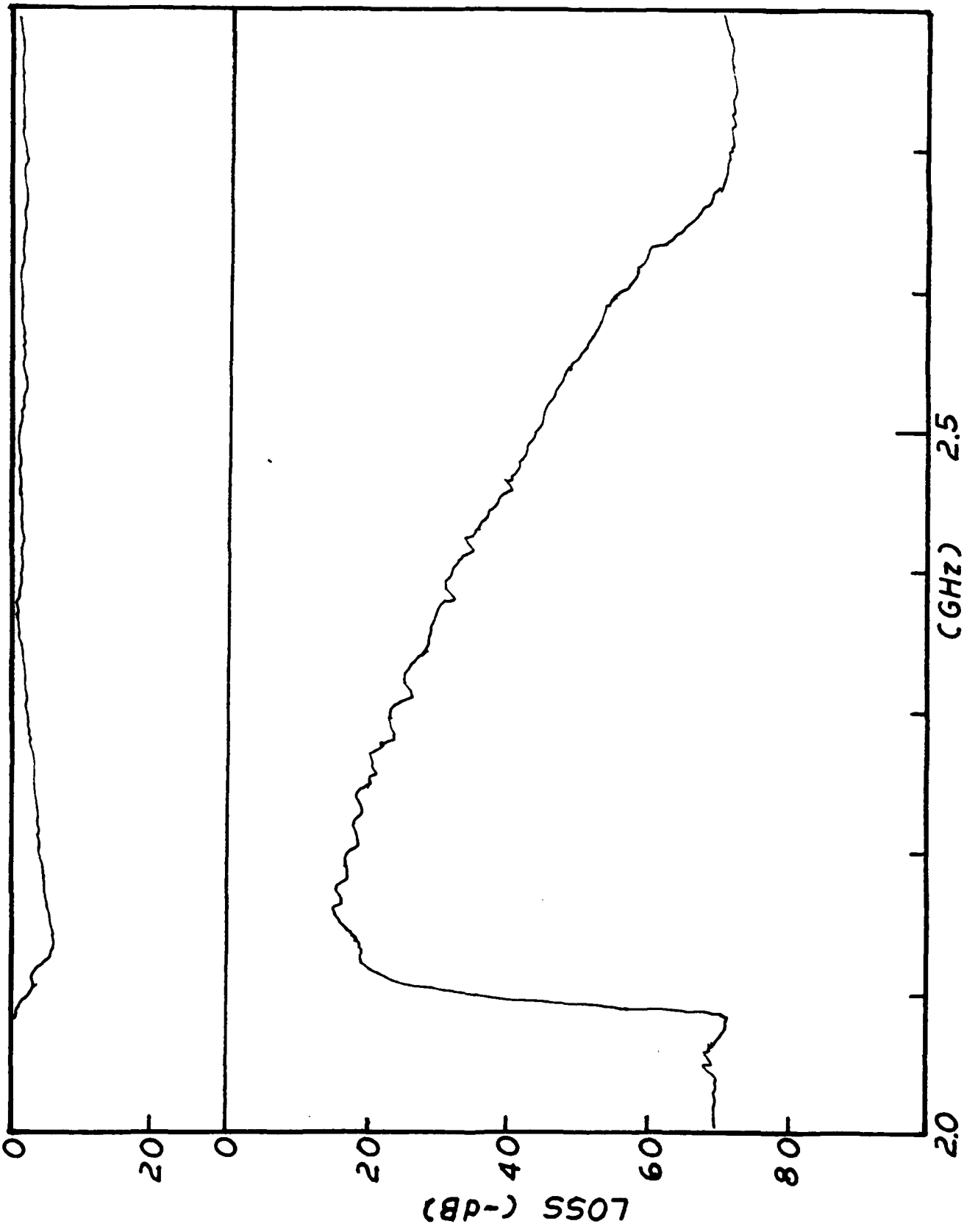

Fig. 9 MSW measurements made on YIG film that worked well in MSW device.

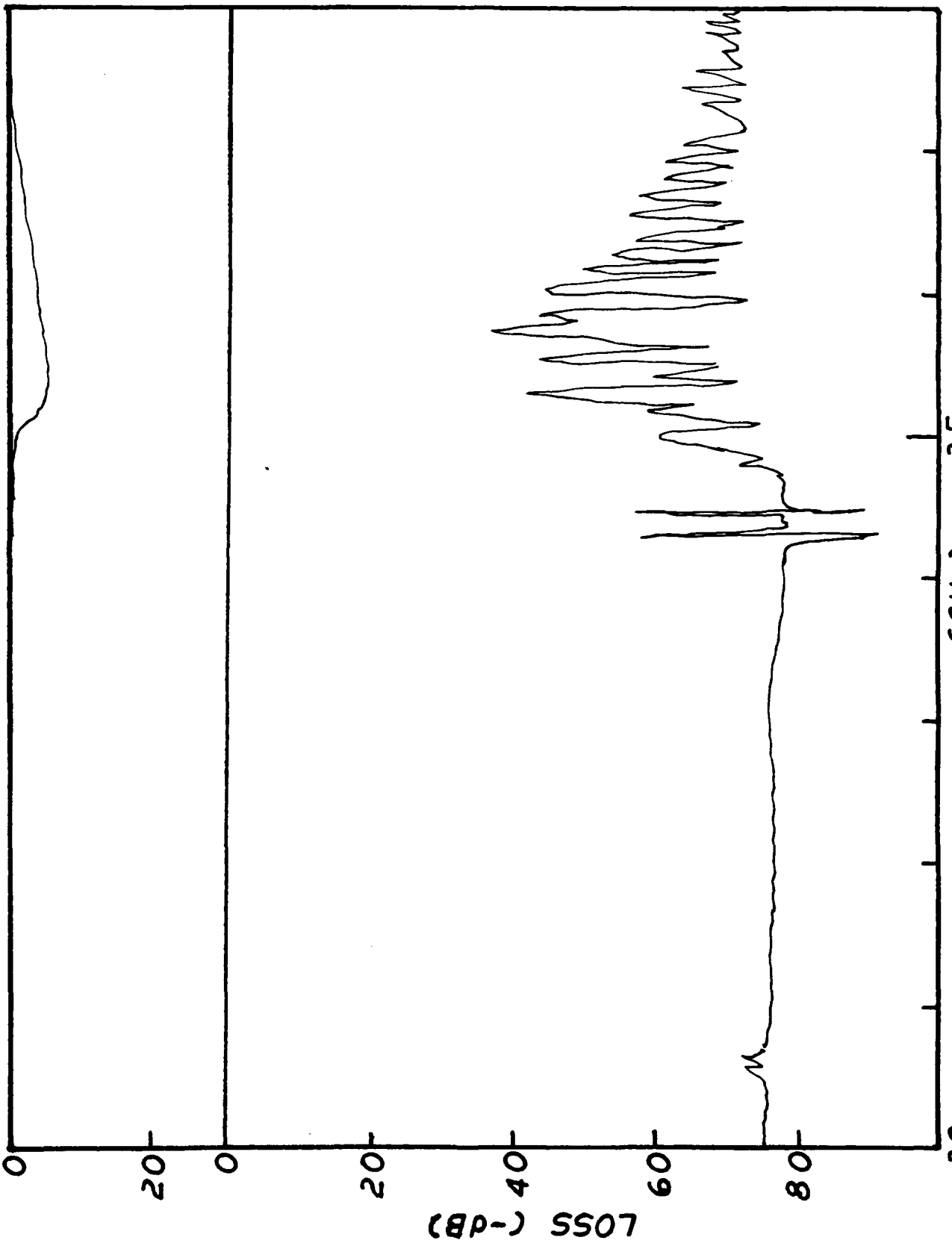

Fig. 10 Passband of film DD-33 as grown.

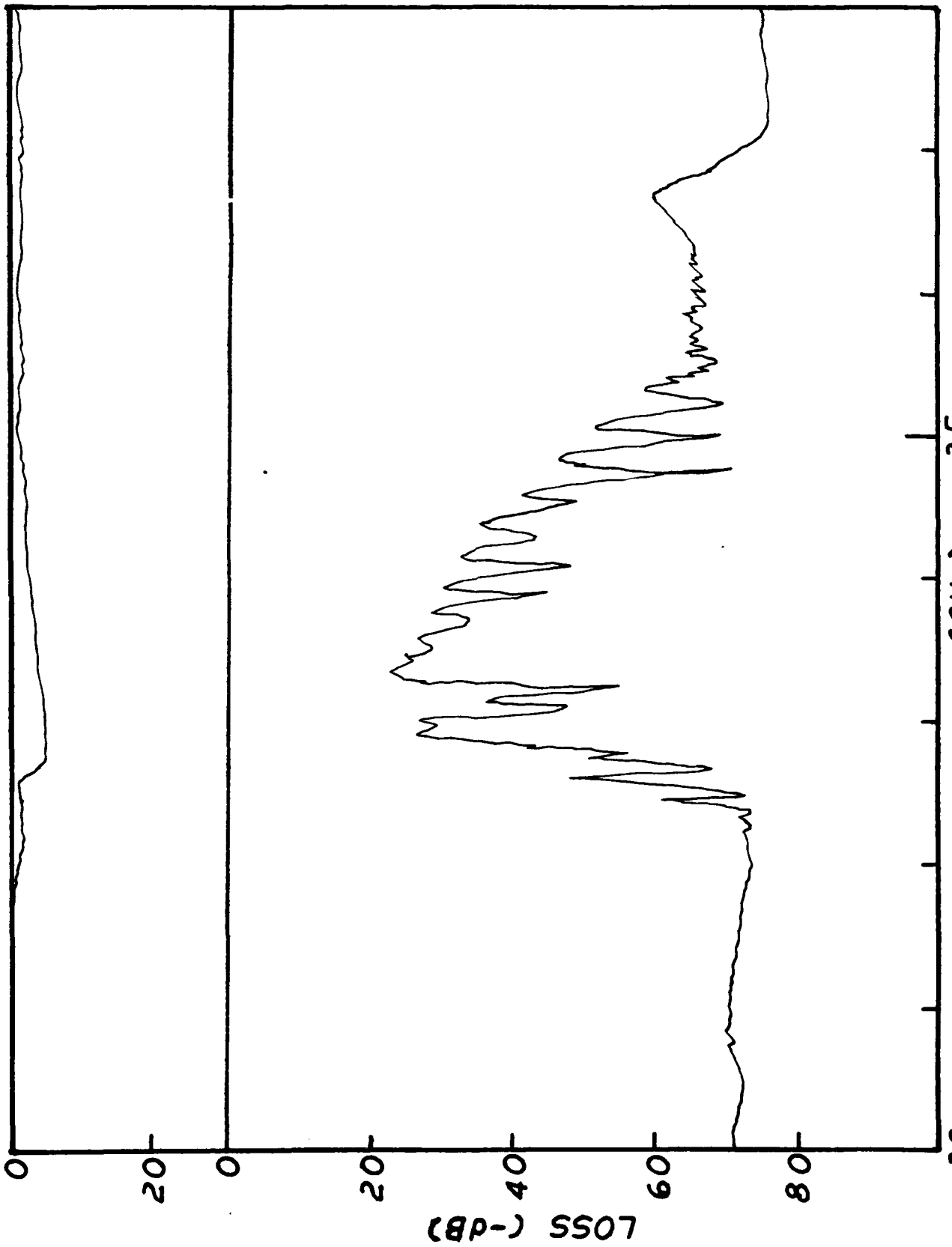

Fig. 11 Passband of film DD-33 after 0.3μm was etched off.

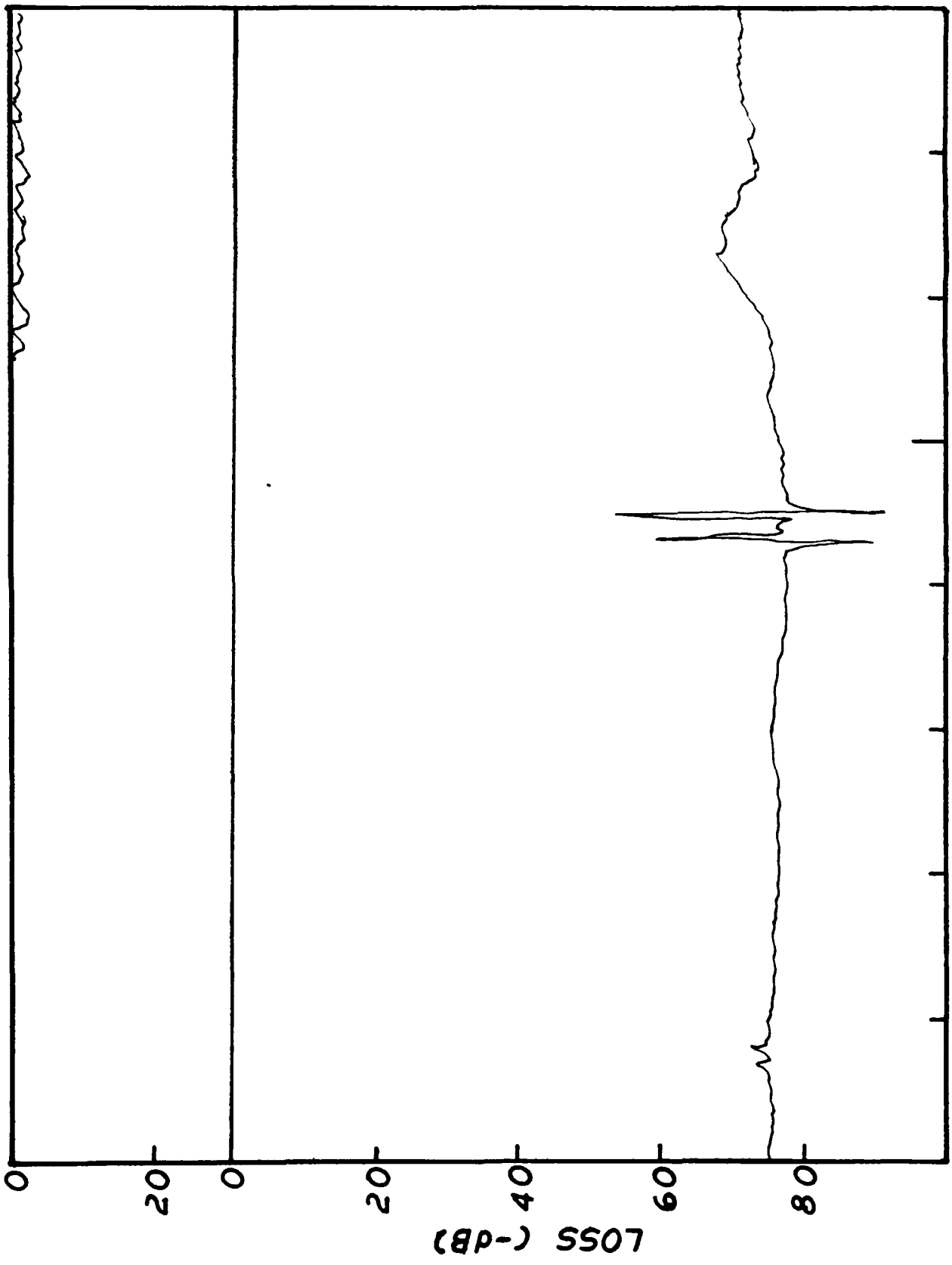

Fig. 12 Passband of film DD-49.

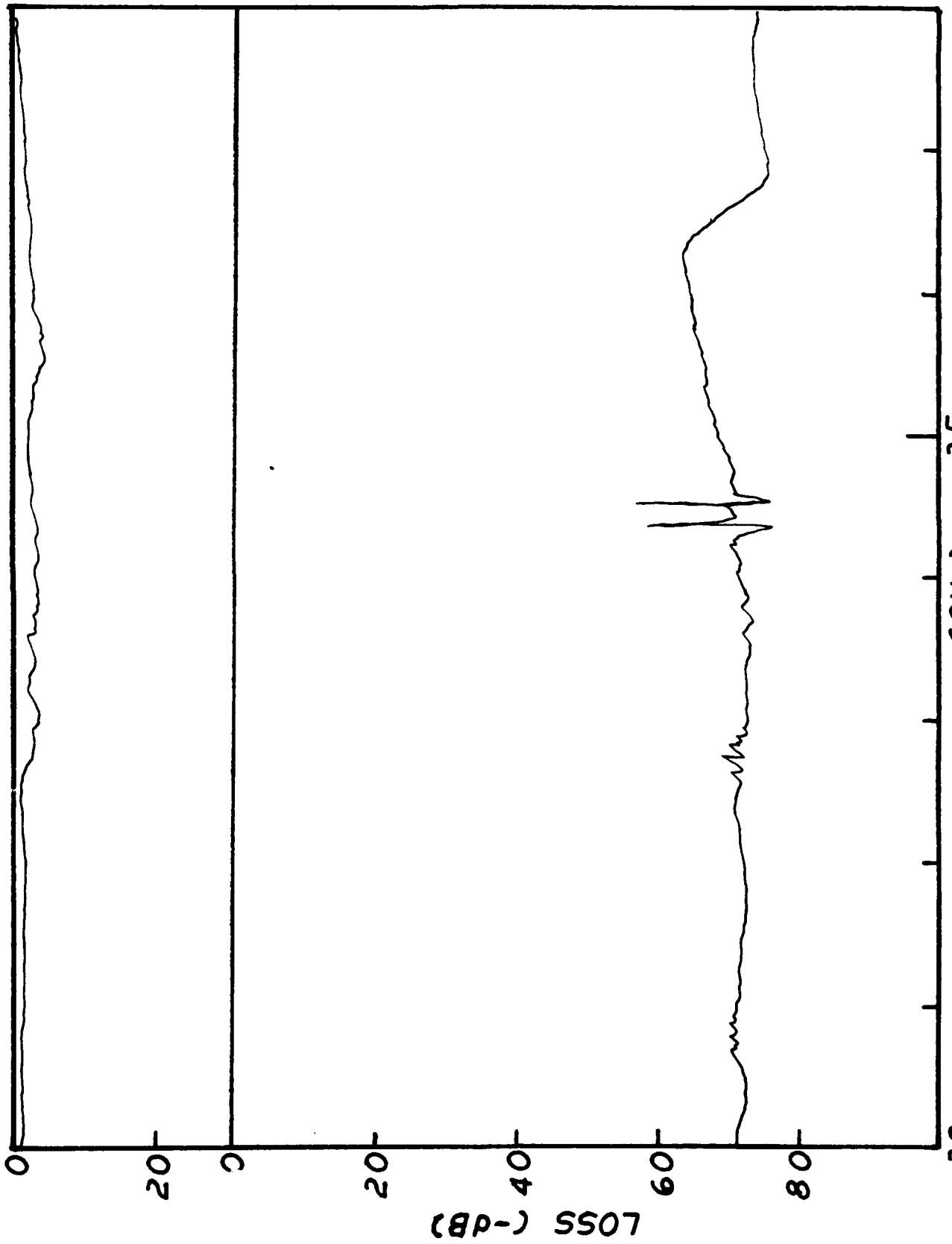

Fig. 13 Passband of film DD-49 after 0.1μm was etched off.

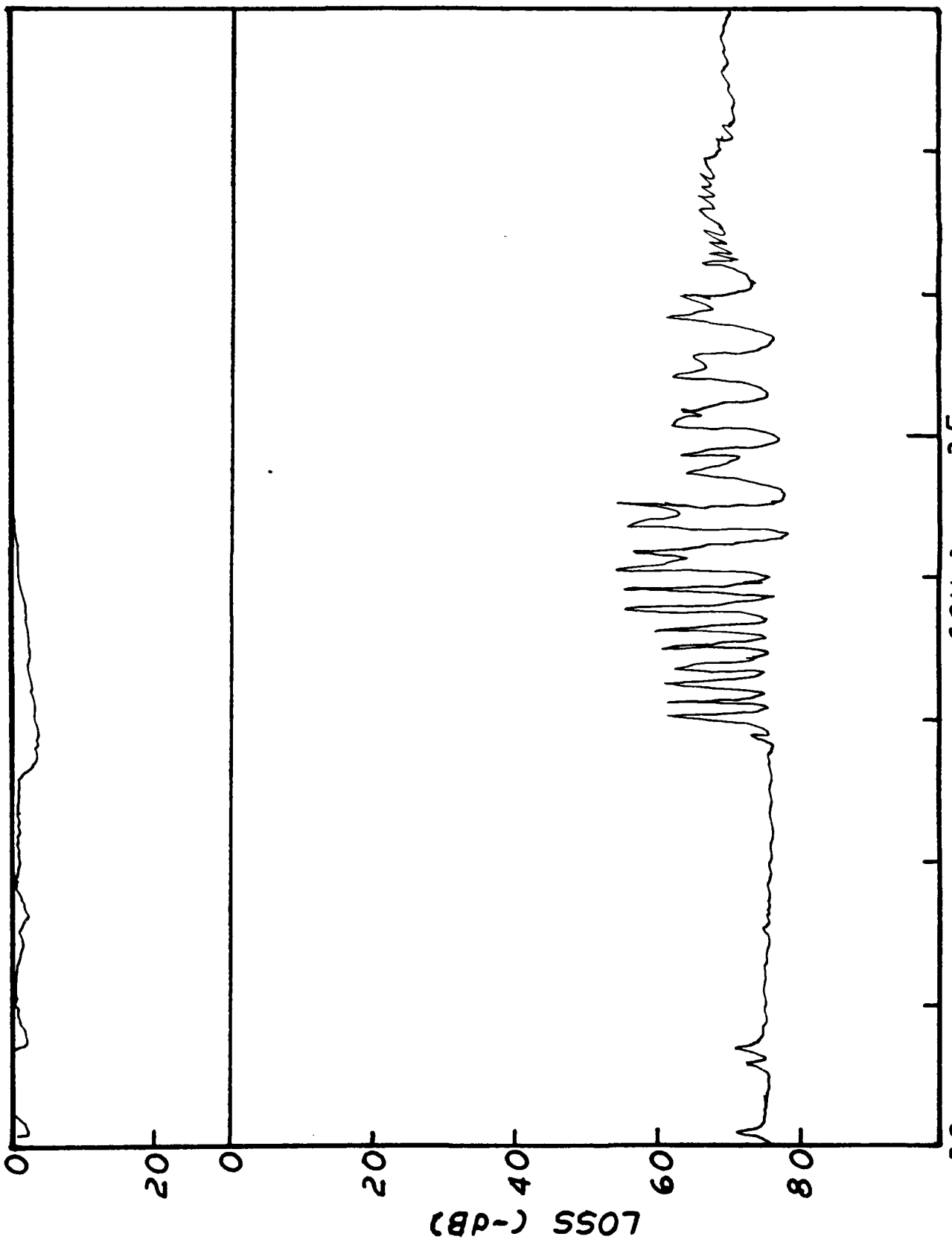

Fig. 14 FMR passband of film DD-10 before annealing.

bismuth in these films such as the development of a wider transition layer than is present in YIG. Discussion of the presence of transition layer and its possible effect on passbands can be found in Adam, et. al.[17]. Another possibility exists however.

Given the fact that only a small section of one film grown by Tamada [18] had a good passband and one film grown in this study (DD-33) after 0.3μm was etched off the outer film surface had a fair passband. The clue may lie in the condition of the outer most layer of film as suggested by Adam.[17] A major difference between the bismuth containing magneto-optic film grown from the Bi_2O_3-Na_2O flux and YIG grown from a PbO-B_2O_3 flux is in the wettability of the flux on the film. Bi_2O_3-Na_2O flux completely wets the film. As the film is withdrawn from the melt, excess flux was spun off but 1/2mm or so of flux still remains. It is known from the growth of $Bi_{0.8}Tm_{0.14}Pb_{0.06}Fe_{3.1}Ga_{1.9}O_{12}$ thin films for aircraft crack detection devices done in this laboratory that about 0.5μm of extra film grows under the flux layer upon extracting the film from the melt. In the $(BiTm)_3(FeGa)_5O_{12}$ films this layer has a different lattice constant from the bulk depending on the cool down rate. When films are cooled very slowly the outer layer of film can be substantially in tension. When very rapidly cooled the film is usually 0.002 A in compression. According to Adam [17] the formation of an outer film layer could cause coupling of the magneto static waves to the spin wave modes. One solution to this is to polish or etch off at least 0.5μm of film. This was substantiated by the improvement in passband of film DD-33 before and after removing 0.3μm (Figures 10 and 11) compared to no change in passband with film DD-49 when only 0.1μm was removed. The poor performance of films grown from the Bi_2O_3 flux (Figures 12 and 13) could be due to the fact that this flux badly damaged the outer surface of the film by ripping out circa 10μm chunks out of the film surface. In contrast YIG films grown from a PbO-B_2O_3 flux when the flux is completely non wetting do not experience this continued growth during film extraction from the furnace. When it was realized that the films grown in this study used a slow pull up procedure it

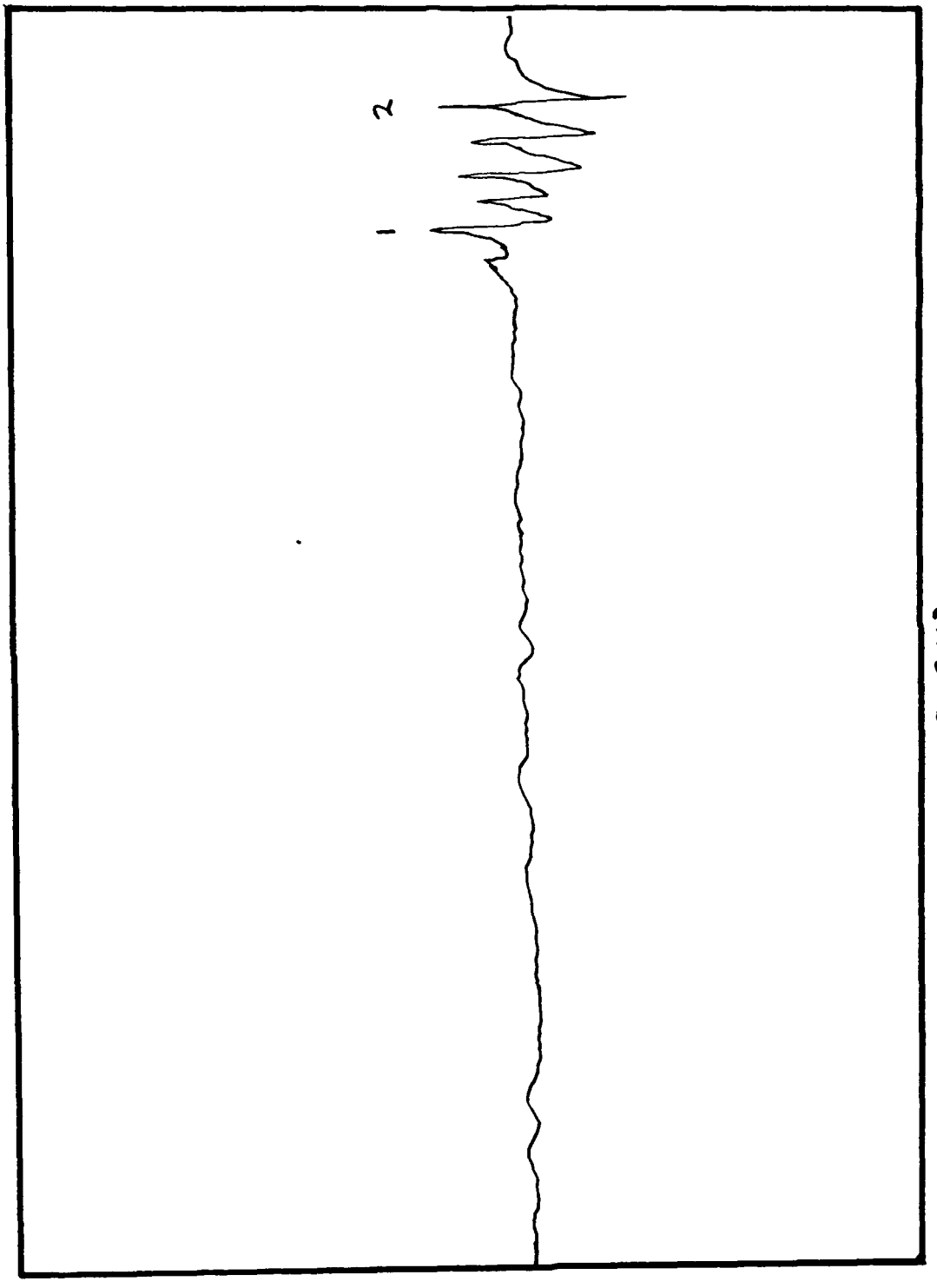

Fig. 15 FMR spectra on film AA-144 over 500 Oe field range.

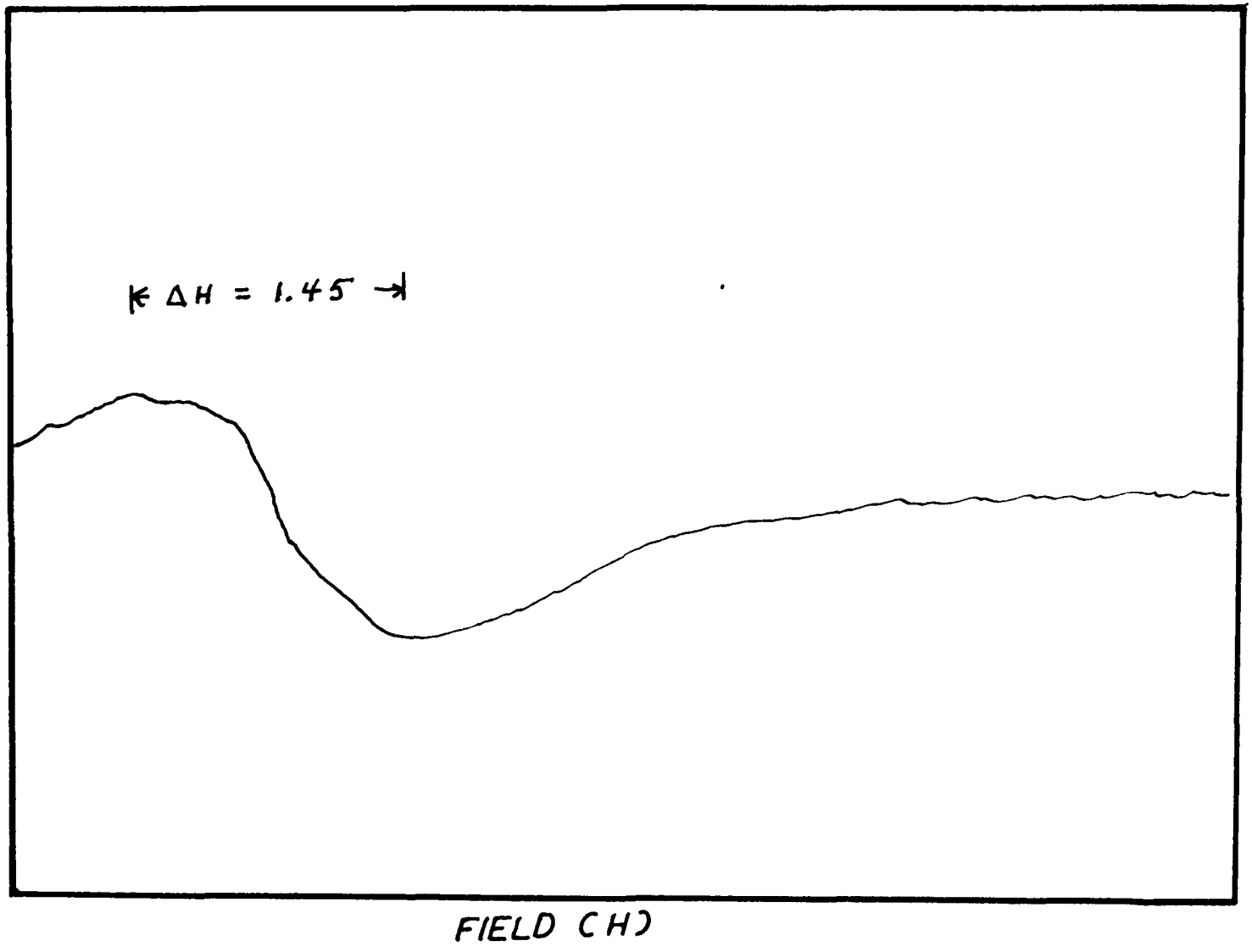

Fig. 16 FMR spectra of peak #1 of Fig. 15 showing linewidth of 1.5 Oe.

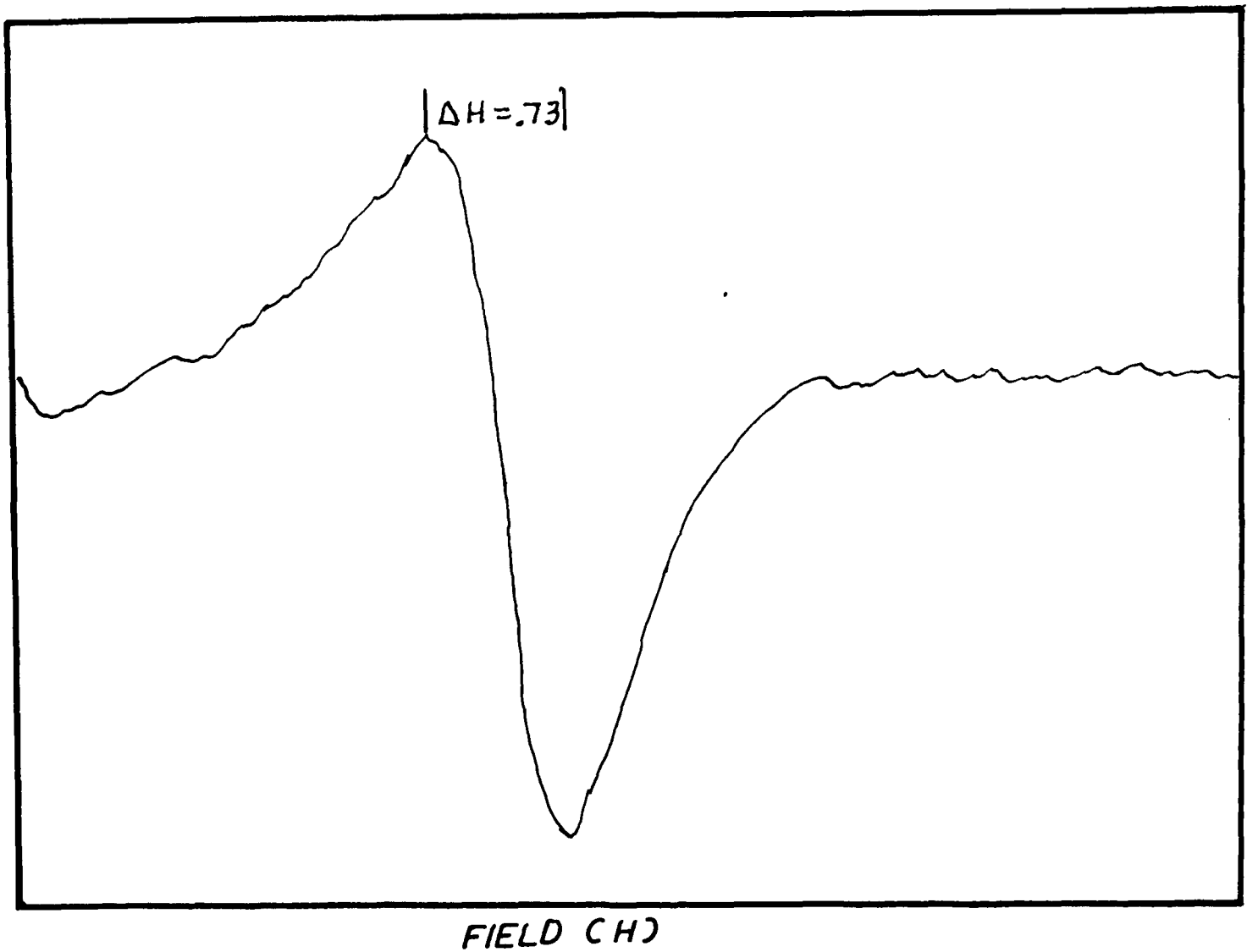

Fig. 17 FMR spectra of peak #2 of Fig. 15 showing linewidth of 0.7 Oe.

would be prudent to polish off 0.5 to 1μm of film of the films and retest the passband. Etching the film surface is not recommended as the size of any growth defect or subsurface damage encountered during handling the film would get larger upon etching. The last film growth run made under our program used the highest purity starting materials available. The compositional data are recorded in Table 8 where again the MgO was added to reduce optical loss. Seven films were grown with the measured properties listed in Table 9. Thicknesses of 1-2μm were desired but they were very difficult to control with the viscous Bi_2O_3 since the film continues to grow in the presence of flux even after extraction from the melt. A low growth rate was also chosen in order to get high film quality. All films were grown with an X-ray lattice constant mismatch in high compression. This was done to introduce the maximum amount of Bi^{3+} into the film for high Faraday rotation. An approximate value for x in the formula $Bi_{3-x}Lu_xFe_5O_{12}$ can be obtained from lattice constant data. For a compression of 0.07 A, x is around 1.55 while at lattice match (12.383A) x is 2.17. At the writing of this report, no data were available on the microwave passbands.

4.0 Conclusions

A thorough study was made on the growth of one inch diameter films of $Bi_{3-x}Lu_xFe_5O_{12}$ on GGG. The introduction of Mg^{2+} provided low attenuation in the near infrared coupled with low ΔH. Particular difficulties were experienced with Bi_2O_3 fluxes for solvents. Inclusions of Pt and orthoferrites, flux adhesion to the surface, and ordinary defects were circumvented to give high quality films. In spite of these precautions, poor MSW passbands were obtained with these films. Attention was devoted to growth rate of films. No firm conclusions could be correlated with rate or speculative transition layers. Efforts were devoted finally to obtain the best overall film quality, both internal and free of surface faults. Even the films with the best surfaces failed to give good passbands. Since the MSW waves are bulk volume waves, it is thought that some unknown defects, arising uniquely from Bi_2O_3 fluxes, must still

Table 8 Melt Composition for Final Growth Run

Chemical	Amount (g)	Purity (%)
Bi_2O_3	745.0	99.999
Na_2CO_3	51.6	99.999
Fe_2O_3	46.1	99.999
Lu_2O_3	9.6	99.999
MgO	0.26	99.999

Table 9 Properties of Grown Films

Film Number	X-ray Mismatch (A) [a]	Film Thickness (μm)	Growth Rate (μm/min)
KK-37	0.065C	6.00	0.85
KK-38	0.076	2.70	1.3
KK-43	0.085	2.00	1.0
KK-44	0.072	1.10	0.5
KK-45	0.064	0.85	0.4
KK-46	0.030	0.94	0.2
KK-47	0.062	1.60	0.2

(a) All films were in compression, i.e., $a_f > a_s$ where a_f is the film and a_s is the substrate lattice constant.

contribute to quality problems in spite of low ΔH values. Our data are consistent with other workers who prepared these films.

5.0 Recommendations

The failure of high quality films to give good MSW passbands has been a minor disappointment. It is difficult to recommend the growth of more films. It would be more fruitful to examine current films for growth anomalies such as defects, layers, or discontinuities in structure. These must be unique to the use of the Bi_2O_3 fluxes and of course have little or no influence on the resonance linewidth. The loss mechanisms in the Bi-Lu films must be different from those in pure YIG films. It points out the fact that MSW wave propagation and the device physics are quite complicated and need to be examined further before applications for channelizers are considered.

6.0 Acknowledgments

The authors thank a number of individuals who through their direct contributions of measurements, suggestions, or discussions have assisted in a partial understanding of new MSW garnet materials. We mention Dr. J.N. Lee of the Naval Research Laboratory who originated the problem. Dr. John C. Butler and Professor J.J. Kramer did numerous physical or microwave measurements. The group at Westinghouse Research Laboratory consisting of Dr. S. Talisa, Dr. J. Adam, and Dr. K. Ju also checked many samples for passband data.

7.0 References

1. G.W. Anderson, D.C. Webb, A.E. Spezio, and J.N. Lee, Proc. IEEE 79, 355 (1991).

2. J.D. Adam in "Physics of Thin Films" Vol. 5, Academic Press, 1991 Edited by M.H. Franiombe and J. Vassen.

3. A.D. Fisher, J.N. Lee, E.S. Gaynor, and A.B. Tveten, Appl. Phys. Lett., 41, 779 (1982).

4. H. Tamada, M. Kaneko, and T. Okamoto, J. Appl. Phys. 64, 554 (1988).

5. J.C. Butler, J.J. Kramer, R.D. Esman, A.E. Craig, J.N. Lee, and T. Ryuo, J. Appl. Phys. 67, 4938 (1990).

6. R. Belt, and J. Ings, SPIE 753, 142 (1987).

7. R.M. Josephs, Proceedings of the AIP 18th Annual Conference on Magnetism and Magnetic Materials, 1972 pp. 283-303/

8. S. Takeda, IEEE Trans. MAG-23, 3340 (1987).

9 H. Takeuchi, S. Ito, I. Mikami, and S. Taniguchi, J. Appl. Phys. 4, 4789 (1973).

10. H. Tamada, and M. Saitoh, J. Appl. Phys. 50, 2446 (1979).

11. J. Adam, T. O'Keefe, and R. Patterson, J. Appl. Phys. 50, 2446 (1979).

12. H. Huahui, S. Hanming, Z. Chengde, and I. Zekun, 1989 Intermag Conference in Washington, D.C., March 27-29, 1989.

13. R. Belt, and J. Ings, J. Appl. Phys. 70, 6398 (1991).

14. H. Tamada, M. Kaneko, and T. Okamoto, J. Appl. Phys. 64, 554 (1988).

15. W. Roode, and J. Robertson, J. Crystal Growth 63, 105 (1983).

16. H. Tamada, and M. Saitoh, J. Appl. Phys. 67, 949 (1990).

17. J. Adam. S. Talisa, J. Kerestes, IEEE Trans. on Magnetics, 25 3488 (1989).

18. Private communications with H. Tamada.

Distribution List

1.	Mr. A.F. Guida Contracting Office, Code 3220 Naval Research Laboratory 4555 Overlook Ave, SW Washington, DC 20375-5000	1
2.	Director, Code 2627 Naval Research Laboratory 4555 Overlook Ave, SW Washington, DC 20375-5000	2
3.	Defense Technical Information Center Building 5, Cameron Station Alexandria, VA 22304-6145	12
4.	Dr. John N. Lee, Code 6537 Naval Research Laboratory 4555 Overlook Ave, SW Washington, DC 20375-5000	6
5.	Professor John Kramer Department of Electrical Engineering University of Delaware Newark, Delaware 19716	2
6.	Dr. John Butler US Army CRDEC SNCCR/DDT ATTN: UV-LIDAR Aberdeen Proving Ground, MD 21010	2
7.	Dr. Sal Talisa Westinghouse Research Center 1310 Beulah Rd Pittsburgh, PA 15235	3
8.	Larry Hucsko, ACO DCASMA Springfield 240 Route 22 Springfield, NJ 07081-3170	2
9.	Prof. Kenneth Tsai Department of Electrical Engineering University of California at Irvine Irvine, Ca 92717	1
10.	Professor Joseph O. Artman Department of Electrical Engineering Carnegie Mellon University Pittsburgh, PA 15213	1